

## GENE THERAPY

## Gene therapy for Wiskott-Aldrich syndrome in a severely affected adult

Emma C. Morris,<sup>1,2</sup> Thomas Fox,<sup>1</sup> Ronjon Chakraverty,<sup>3,4</sup> Rita Tendeiro,<sup>1</sup> Katie Snell,<sup>5,6</sup> Christine Rivat,<sup>5</sup> Sarah Grace,<sup>3</sup> Kimberly Gilmour,<sup>6</sup> Sarita Workman,<sup>2</sup> Karen Buckland,<sup>5</sup> Katie Butler,<sup>5</sup> Ronnie Chee,<sup>2</sup> Alan D. Salama,<sup>7</sup> Hazem Ibrahim,<sup>8</sup> Havinder Hara,<sup>5</sup> Cecile Duret,<sup>5</sup> Fulvio Mavilio,<sup>9</sup> Frances Male,<sup>10</sup> Frederick D. Bushman,<sup>10</sup> Anne Galy,<sup>9</sup> Siobhan O. Burns,<sup>1,2</sup> H. Bobby Gaspar,<sup>5,6,\*</sup> and Adrian J. Thrasher<sup>5,6,\*</sup>

<sup>1</sup>Institute of Immunity and Transplantation, University College London, London, United Kingdom; <sup>2</sup>Department of Immunology and <sup>3</sup>Department of Haematology, Royal Free London NHS Foundation Trust, London, United Kingdom; <sup>4</sup>Cancer Institute, University College London, London, United Kingdom; <sup>5</sup>Institute of Child Health, University College London, London, United Kingdom; <sup>6</sup>Great Ormond Street Hospital for Children NHS Foundation Trust, London, United Kingdom; <sup>7</sup>Centre for Nephrology, University College London, London, United Kingdom; <sup>8</sup>Department of Histopathology, Royal Free London NHS Foundation Trust, London, United Kingdom; <sup>9</sup>Genethon, Evry, France; and <sup>10</sup>Department of Microbiology, University of Pennsylvania School of Medicine, Philadelphia, PA

## Key Points

- We describe the first successful use of gene therapy in a severely affected adult with WAS.
- Gene therapy is a viable strategy for adult WAS patients with severe chronic disease complications where allogeneic transplantation presents.

Until recently, hematopoietic stem cell transplantation was the only curative option for Wiskott-Aldrich syndrome (WAS). The first attempts at gene therapy for WAS using a  $\gamma$ -retroviral vector improved immunological parameters substantially but were complicated by acute leukemia as a result of insertional mutagenesis in a high proportion of patients. More recently, treatment of children with a state-of-the-art self-inactivating lentiviral vector (LV-w1.6 WASp) has resulted in significant clinical benefit without inducing selection of clones harboring integrations near oncogenes. Here, we describe a case of a presplenectomized 30-year-old patient with severe WAS manifesting as cutaneous vasculitis, inflammatory arthropathy, intermittent polyclonal lymphoproliferation, and significant chronic kidney disease and requiring long-term immunosuppressive treatment. Following reduced-intensity conditioning, there was rapid engraftment and expansion of a polyclonal pool of transgene-positive functional T cells and sustained gene marking in myeloid and B-cell lineages up to 20 months of observation. The patient was able to discontinue immunosuppression and exogenous immunoglobulin support, with improvement in vasculitic disease and proin-

flammatory markers. Autologous gene therapy using a lentiviral vector is a viable strategy for adult WAS patients with severe chronic disease complications and for whom an allogeneic procedure could present an unacceptable risk. This trial was registered at [www.clinicaltrials.gov](http://www.clinicaltrials.gov) as #NCT01347242. (*Blood*. 2017;130(11):1327-1335)

## Introduction

Wiskott-Aldrich syndrome (WAS) is a rare, X-linked, complex primary immunodeficiency disease caused by mutations in the WAS gene which encodes a 502-amino-acid protein called the Wiskott-Aldrich protein (WASp). This regulates the actin cytoskeleton in most hematopoietic lineages and is consequently important for normal function of many immunological processes.<sup>1-4</sup> Clinical and biological manifestations of WAS include microthrombocytopenia, recurrent infections, and eczema. Patients also display an increased incidence of autoimmunity and are at risk of developing lymphoproliferative disorders and lymphoid malignancies.<sup>5</sup> A clinical scoring system grades disease severity. Patients with a score of 3 to 5 display “classical” WAS, usually as a result of null mutations. Without definitive treatment, these patients are not normally expected to survive beyond their third decade.<sup>6</sup> For many years, the only potential curative therapy has been allogeneic hematopoietic stem cell transplantation (HSCT).<sup>7-9</sup> HLA-matched HSCT is today associated with high rates of survival, but HLA-mismatched HSCT may still be

accompanied by unacceptable risk in some cases, even though new immune cell-depletion technologies are promising for reduction of graft-versus-host disease and acceleration of immunological reconstitution.<sup>10,11</sup>

Gene therapy (GT) for WAS was first attempted using a  $\gamma$ -retroviral vector.<sup>12</sup> This approach resulted in a sustained increase in the proportion of WASp-corrected cells in all patients. However, 7 of the 9 treated patients developed acute leukemia secondary to viral enhancer-mediated insertional mutagenesis. More recently, GT using a self-inactivating lentiviral vector has shown promise in children.<sup>13,14</sup> Interim analysis of results from both studies has demonstrated significant clinical benefit and, importantly, without evidence of oncogenic transformation or sustained clonal dominance.

Here, we describe a case of an adult WAS patient (aged 30 years) for whom an HLA-matched donor could not be found and a T-cell receptor (TCR)  $\alpha\beta$ -depleted haploidentical transplant was deemed to be excessively high risk as a result of significant preexisting

Submitted 4 April 2017; accepted 4 July 2017. Prepublished online as *Blood* First Edition paper, 17 July 2017; DOI 10.1182/blood-2017-04-777136.

\*H.B.G. and A.J.T. contributed equally to this study.

The online version of this article contains a data supplement.

There is an Inside *Blood* Commentary on this article in this issue.

The publication costs of this article were defrayed in part by page charge payment. Therefore, and solely to indicate this fact, this article is hereby marked “advertisement” in accordance with 18 USC section 1734.

© 2017 by The American Society of Hematology

**Table 1. T-cell proliferation assays, lymphocyte subsets, and vaccination responses before and after GT**

	Before GT	After GT	Healthy control ranges for 3-d stimulation
<b>T-cell proliferation</b>			
Spontaneous (cpm)	103	115*	
PHA (cpm)	2490	50 349*	18 906-417 388
aCD3 (cpm)	226	22 699*	187-122 682
aCD3/aCD28 (cpm)	2186	52 068*	1202-213 904
<b>Lymphocyte subsets</b>			
Total lymphocytes ( $\times 10^9$ /mL) (normal range: 1.0-2.8)	0.572	2.251†	1.469/1.11§
CD3 ( $\times 10^9$ /mL) (normal range: 0.7-2.1)	0.518	1.389†	0.789/0.723§
CD4 ( $\times 10^9$ /mL) (normal range: 0.3-1.4)	0.414	0.62†	0.407/0.409§
CD8 ( $\times 10^9$ /mL) (normal range: 0.2-0.9)	0.105	0.408†	0.252/0.23§
CD19 ( $\times 10^9$ /mL) (normal range: 0.1-0.5)	0.027	0.408†	0.407/0.409§
<b>Vaccination responses</b>			
Total pneumococcal titres (mg/L) (protective levels >20 mg/L)	On immunoglobulin replacement therapy	4‡	43
Pneumococcus serotype-specific responses (protective levels >0.35 mg/L)	On immunoglobulin replacement therapy	ND‡	Protective responses against 3/13 serotypes
Tetanus toxoid (IU/mL) (protective levels: 0.1-0.7)	On immunoglobulin replacement therapy	0.14‡	2.51

PHA, phytohemagglutinin.

\*16 months after GT.

†6 months after GT.

‡After GT, before vaccination.

§11 months/16 months after GT.

||After GT, after vaccination.

disease comorbidities. The patient was successfully treated on trial (NCT01347242) with GT using the same self-inactivating vector (LV-w1.6 WASp), which had previously recruited only children.<sup>14</sup>

## Methods

### Clinical protocol

The patient was managed under the care of the clinical immunology and adult bone marrow transplant services at the Royal Free London Hospital NHS Foundation Trust (London, England). The patient was treated on trial (#NCT01347242) sponsored by Genethon.<sup>14</sup> The trial protocol was approved by the UK Medicines and Healthcare Products Regulatory Agency, Gene Therapy Advisory Committee, and the National Research Ethics Service. Autologous hematopoietic stem cells were collected from mobilized peripheral blood (after cryopreservation of an unmodified back up stem cell harvest) and were genetically modified ex vivo during concurrent reduced-intensity conditioning of the patient, as described below.

He received IV methylprednisolone 70 mg (1 mg/kg) on days -8 to -4 as prophylaxis against a potential granulocyte colony-stimulating factor-induced inflammatory reaction, lenograstim 1.28 million units/kg subcutaneously on days -7 to -5 followed by plerixafor 0.16 mg/kg subcutaneously on days -5 to -4. The patient underwent leukapheresis on days -4 and -3. Following confirmation of an adequate starting dose of CD34<sup>+</sup> cells, conditioning was commenced as per protocol with fludarabine 40 mg/m<sup>2</sup> daily (days -3 to -1) and busulfan 3.2 mg/kg daily (days -3 to -1). No adjuvant serotherapy was given. Due to the patient's poor renal function (EDTA glomerular filtration rate, 34 mL/min), prophylactic hemodialysis was undertaken on day 0. The patient was already established on antibacterial prophylaxis with penicillin V and IV immunoglobulin following the earlier splenectomy, and this was continued. Antifungal prophylaxis with voriconazole was commenced on day +3, and antiviral prophylaxis with acyclovir was started on admission at day -9. Oral trimethoprim-sulfamethoxazole 3 times a week was used as *Pneumocystis jirovecii* prophylaxis from day -9.

On day 0, transduced autologous CD34<sup>+</sup> hematopoietic stem cells were infused. The patient received a total dose of CD34<sup>+</sup> cells of  $3.77 \times 10^6$ /kg, with a 52% transduction efficiency as determined by flow cytometry (gating on CD34<sup>+</sup>, CD45<sup>+</sup> cells). The transduced cell products were manufactured at Great Ormond Street Hospital (London, England). Vector production, biological analyses,

CD34<sup>+</sup> cell gene transfer procedure, integration site analysis, and clonality assays were performed as previously described.<sup>14</sup> The manufacturing process is further outlined below.

### Vector production

The clinical LV-w1.6 WASp vector is an advanced generation HIV-derived lentiviral vector pseudotyped with VSVg and expressing the full-length WAS complementary DNA from the WAS gene proximal 1.6-kb promoter. The clinical vector batch was manufactured at Genethon (Evry, France). Batches were purified, concentrated, and titered for infectious particles (infectious genomes per milliliter) as previously reported.<sup>14</sup>

### CD34<sup>+</sup> cell gene transfer procedure

Cells were cultured at  $1 \times 10^6$  cells/mL in tissue culture-treated flasks (NUNC) in serum-free medium (X-vivo 20, Lonza) and animal-free stem cell factor

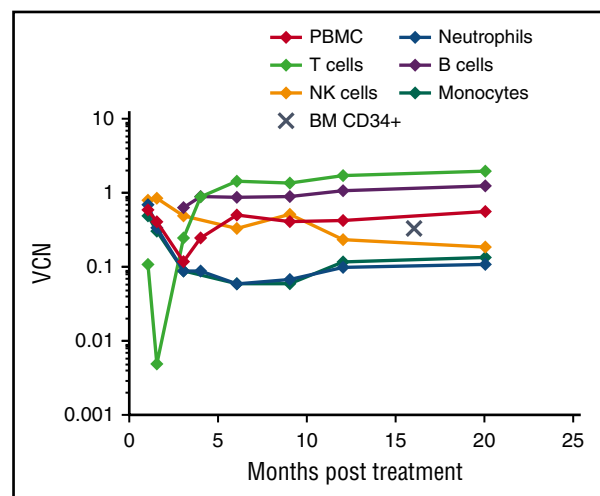
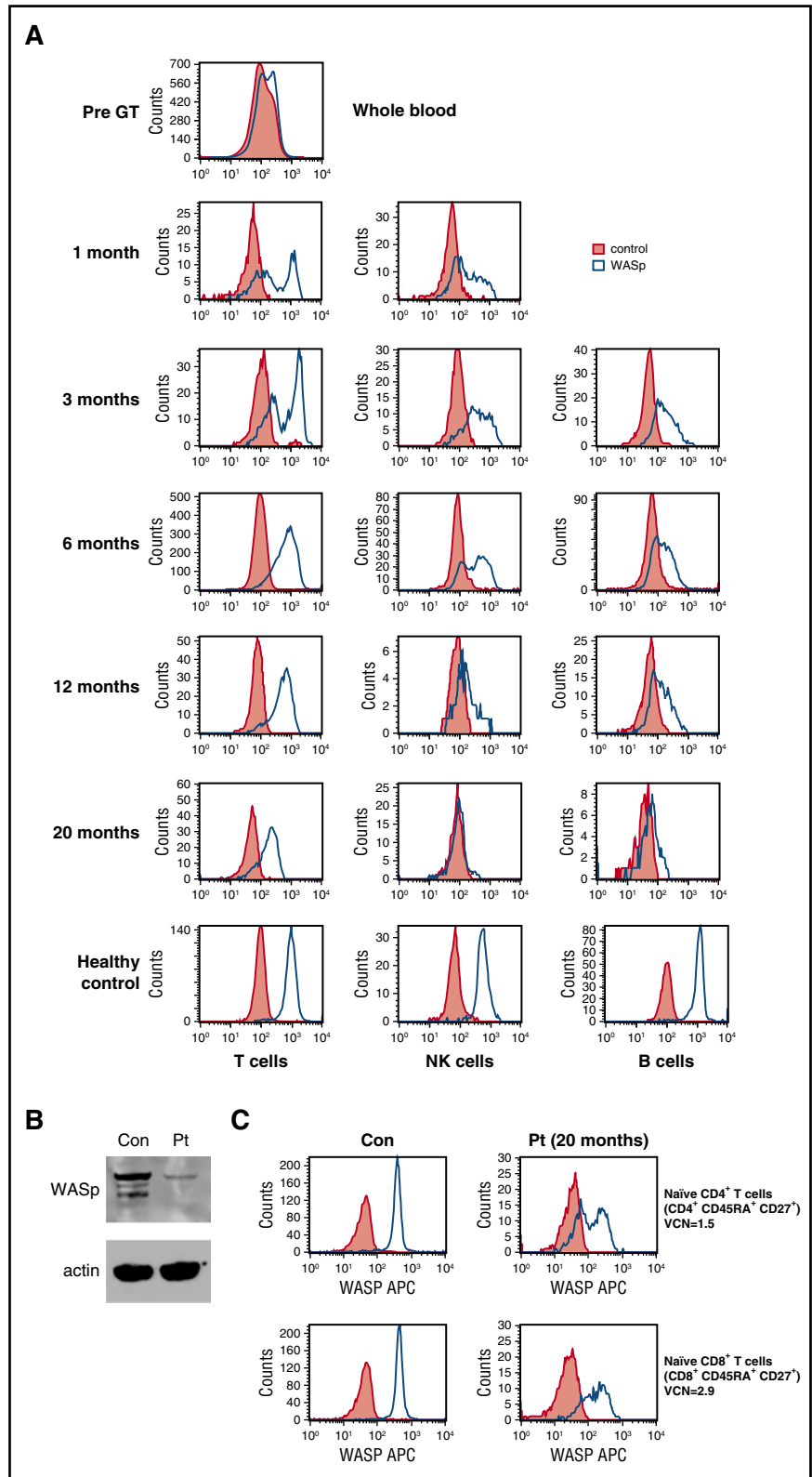


**Figure 1. Persistent gene marking post-GT.** Longitudinal results of gene marking in peripheral blood and bone marrow after GT as expressed by vector copy number per PBMC, peripheral blood purified cell lineage, or bone marrow-derived CD34<sup>+</sup> cell. BM, bone marrow; NK, natural killer; VCN, vector copy number.

**Figure 2. Correction of WASp expression post-GT.** (A) WASp protein expression in T cells, B cells, and natural killer cells. (B) Western blot demonstrating WASp expression in the patient's platelets (Pt) compared with a healthy control (con). NB, patient received no platelet transfusions at any time. (C) WASp expression in purified naive CD4<sup>+</sup> and CD8<sup>+</sup> T cells at 20 months post-GT.



(300 ng/mL), Fms-like tyrosine kinase 3 ligand (300 ng/mL), thrombopoietin (100 ng/mL), and interleukin-3 (IL-3; 20 ng/mL) (all from Peprotech). G-CSF and Plerixafluor mobilized peripheral blood was collected from the patient by apheresis. Immunomagnetic beads and an immunomagnetic separation device were used to positively select CD34<sup>+</sup> cells (CliniMACS, Miltenyi Biotec). CD34<sup>+</sup> cells were seeded in serum-free medium (X-Vivo20, Lonza),

supplemented with 1% human albumin solution and the cytokines IL-3, stem cell factor, Fms-like tyrosine kinase 3 ligand, and thrombopoietin. All cytokines (Peprotech) and culture reagents were approved for ex vivo clinical use. Cells were then incubated at 37°C, 5% CO<sub>2</sub>. After 17 hours total prestimulation, cells were returned to precoated tissue culture flasks and transduced twice with LV. w1.6 WASp (2 × 10<sup>8</sup> infectious particles per milliliter) for 17 hours each time.

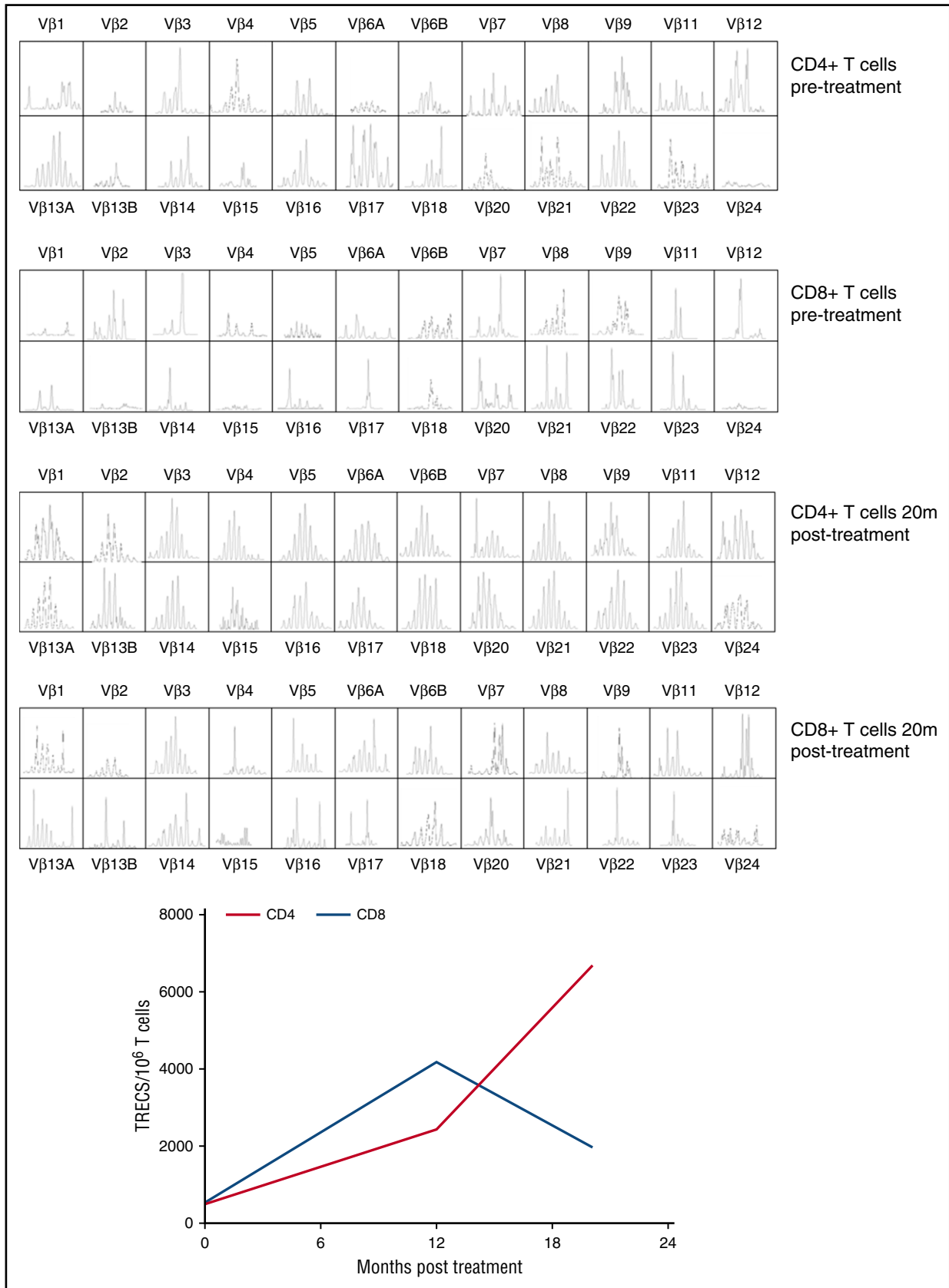


**Figure 3. Improvement of T-cell repertoire and thymic output post-GT.** (A) T-cell repertoire analysis by TCR spectratyping pre- and post-GT in CD4<sup>+</sup> and CD8<sup>+</sup> T cells. (B) sjTREC content in CD4<sup>+</sup> (red line) and CD8<sup>+</sup> (blue line) T cells (dotted line corresponds to the tenth centile for the patient's age group). TRECs, T cell receptor excision circles.

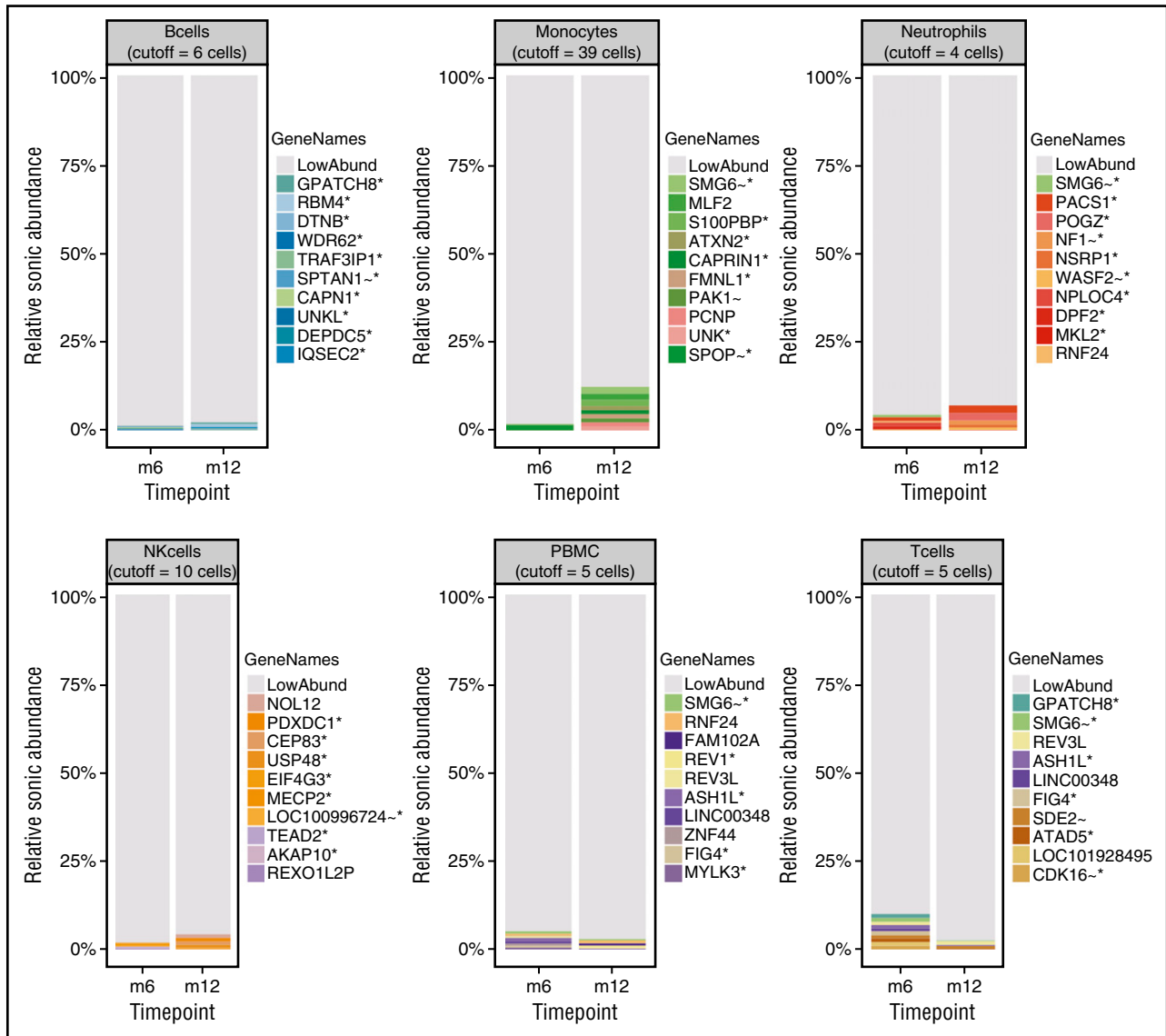


**Figure 4. Relative abundance of cell clones.** Stacked bar graphs showing the relative sonic abundance, scaled as a proportion of the total. Data are separated by cell type with side-by-side comparison of time points for visualization of longitudinal changes. The 10 most abundant integration sites for each cell type are emphasized by uniquely colored bars and named by the nearest gene, indicated in the “GeneNames” key. The genes are marked with symbols to indicate further information about the integration site/gene as follows: \*, the site is within a transcription unit; ~, the site is within 50 kb of a cancer related gene; !, the gene is associated with lymphoid cancers in humans. The remaining low-abundance integration sites are indicated in gray (LowAbund). The cutoff values for binning clones as low abundance are indicated at the top of each cell-type panel.

Washed cells were then resuspended (at  $3 \times 10^6$  CD34<sup>+</sup> cells per milliliter) in 2% human albumin in a sterile bag for infusion to the patient. Reserved cell aliquots were cultured for 14 days afterward to assess proviral integration by quantitative polymerase chain reaction (qPCR) and WASp expression by flow cytometry.

**Analysis of thymic output**

Signal joint TCR excision circles (sjTREC) were assessed using real-time qPCR. sjTREC content was expressed in copies per  $10^5$  peripheral blood mononuclear cells (PBMCs) (control range, 150-2500/ $10^5$  PBMCs).

**T-cell repertoire analysis by TCR spectratyping**

Clonality of T cells was monitored using TCR V  $\beta$  spectratyping. Briefly, the CDR3 region of the  $\beta$  chain was amplified from patient complementary DNA using a single constant region primer with 24 variable region primers. A fluorescent run-off reaction was then carried out, and the products were run on a 3500xL Genetic Analyzer. Subsequent spectratypes were analyzed using

GeneMapper 5 software and flow analysis used the IOTest  $\beta$  Mark assay (Beckman Coulter).

**Analysis of vector copy number**

Vector copy number per cell was measured by qPCR detection of the vector’s HIV  $\psi$  sequence with normalization against the copy number of the albumin gene. Lymphoid and myeloid subpopulations were sorted by flow cytometry using their corresponding fluorescence-labeled monoclonal antibodies.

**Analysis of integration site distributions.** Detailed methods are as described previously.<sup>15-19</sup> Briefly, DNA was randomly sheared via ultrasonication, and DNA linkers were ligated to the cleaved ends. DNA fragments were then amplified by ligation-mediated PCR using primers annealing to the long terminal repeat of the vector and to the linker to isolate and enrich for host-vector junctions. PCR was performed in quadruplicate for each sample. Amplicons were sequenced using an Illumina MiSeq instrument. Sequence reads were aligned to the human genome (hg18) to identify vector integration sites. The

**Table 2. Distribution and relative abundance of integration sites isolated from several cell types 6 and 12 months after therapy**

Time point and cell type	Total reads	Inferred cells	Unique sites	S.chao1	Gini	Shannon	UC50
<b>6 mo</b>							
B cells	1 036 782	4639	3891	19855	0.1204	8.2045	1647
Monocytes	222 125	329	248	893	0.1950	5.4176	86
Neutrophils	803 235	2018	1522	6981	0.1866	7.2162	552
NK cells	1 111 841	3000	2128	7757	0.1751	7.5657	795
PBMC	684 175	2115	1386	4844	0.2668	7.0254	381
T cells	1 038 680	5685	3089	10 815	0.3937	7.4591	539
<b>12 mo</b>							
B cells	925 356	2197	1745	7702	0.1438	7.3907	701
Monocytes	347 061	351	242	1970	0.2517	5.3341	69
Neutrophils	558 321	729	492	1866	0.2496	6.0383	139
NK cells	507 007	697	469	1865	0.2413	6.0123	135
PBMC	463 071	2076	1744	7513	0.1387	7.3578	720
T cells	981 471	3142	2089	9696	0.2748	7.3678	574

The table summarizes the sample metadata and sequencing data and reports summary statistics for each sample. To summarize the data, the total number of sequence reads (total reads), the inferred number of cells with integrated vector identified (inferred cells), and the number of unique integration sites identified (unique sites) are shown. Statistics to summarize population structure are also presented. The Chao1 analysis (S.chao1) is an estimate of minimum population size.<sup>23</sup> The Gini coefficient is a measure to represent distribution. Here, a value of 0 indicates even distribution of integration sites, while values increasing toward 1 demonstrate increasing inequality of integration site abundance within the population. The Shannon index summarizes diversity by accounting for both abundance and evenness among the integration sites in the cell population. Lastly, the UC50, a new metric, indicates the number of unique clones contributing the top 50% of the sample's total abundance.<sup>16</sup>

distance between the vector–host junction and the breakpoint of the DNA produced by shearing can be used to differentiate distinct cells with the same integration site. Since the DNA is randomly sheared via sonication prior to amplification, these DNA fragment lengths, or “sonic lengths,”<sup>19</sup> can be used to estimate the abundance of cell clones, avoiding the need to estimate based on read counts acquired after biased amplification and sequencing. Cells harboring the same integration site can be differentiated and directly counted by sonic length and then summed to estimate the abundance (“sonic abundance”) of the integration site within the population. DNA sequence reads used in this study are available at the National Center for Biotechnology Information Sequence Read Archive under accession number BioProject ID PRJNA387194.

**Analysis of WASp expression.** WASp expression in PBMCs and lymphocytes was analyzed by flow cytometry on a FACSCalibur cell analyzer (BD Biosciences) using the Simultest CD3 fluorescein isothiocyanate/CD16<sup>+</sup>CD56 phycoerythrin and CD19PECy7 antibodies (BD Biosciences) for lymphocyte characterization and the WASp (immunoglobulin G<sub>2a</sub> [IgG<sub>2a</sub>]) 5A5 clone (BD Biosciences) for WASp intracellular staining. For western blotting, platelets were purified from EDTA-blood by serial centrifugation (15 min at 800 rpm with no brake followed by 15 min at 1800 rpm). Protein extracts from the pelleted platelets were separated on a 10% SDS-PAGE gel, and WASp was detected using WASp (D-1) antibody (Santa Cruz Biotechnology).

## Results

### Case presentation

The patient first presented at 3 years of age with easy bruising and epistaxis. Thrombocytopenia and small platelets on peripheral blood film examination raised the suspicion of WAS. Western blotting for WASp and gene sequencing were performed later and confirmed the clinical diagnosis. Sanger sequencing confirmed a T>C mutation 2 bases into the 5' splice site of intron 9 of the WASp gene (IVS9+2 T to C). This mutation is predicted to disrupt the splicing of exon 9 resulting in the activation of a cryptic splice site and the insertion of the 115-bp 5' segment of intron 9 causing a frameshift and a termination codon within the inserted segment.<sup>6,20,21</sup> The patient is of Asian British Pakistani ethnicity, and there were no other documented cases in the patient's family. After episodes of spontaneous bleeding secondary to thrombocytopenia later in childhood, a splenectomy was performed, which resulted in normalization of platelet numbers. In midchildhood, the patient began to develop autoimmune and inflammatory phenomena,

including recurrent episodes of uveitis, cutaneous leukocytoclastic vasculitis with skin ulceration, episodic synovitis, thyroiditis, and nonmalignant lymphoproliferative disease. These episodes were accompanied by gross elevation in acute phase proteins. The vasculitis in particular was increasingly difficult to control and persisted throughout adolescence. Immunosuppression with varying combinations of steroids, colchicine, methotrexate, cyclophosphamide, cyclosporin, mycophenolate mofetil, and rituximab failed to fully control the patient's symptoms or to normalize inflammatory markers.

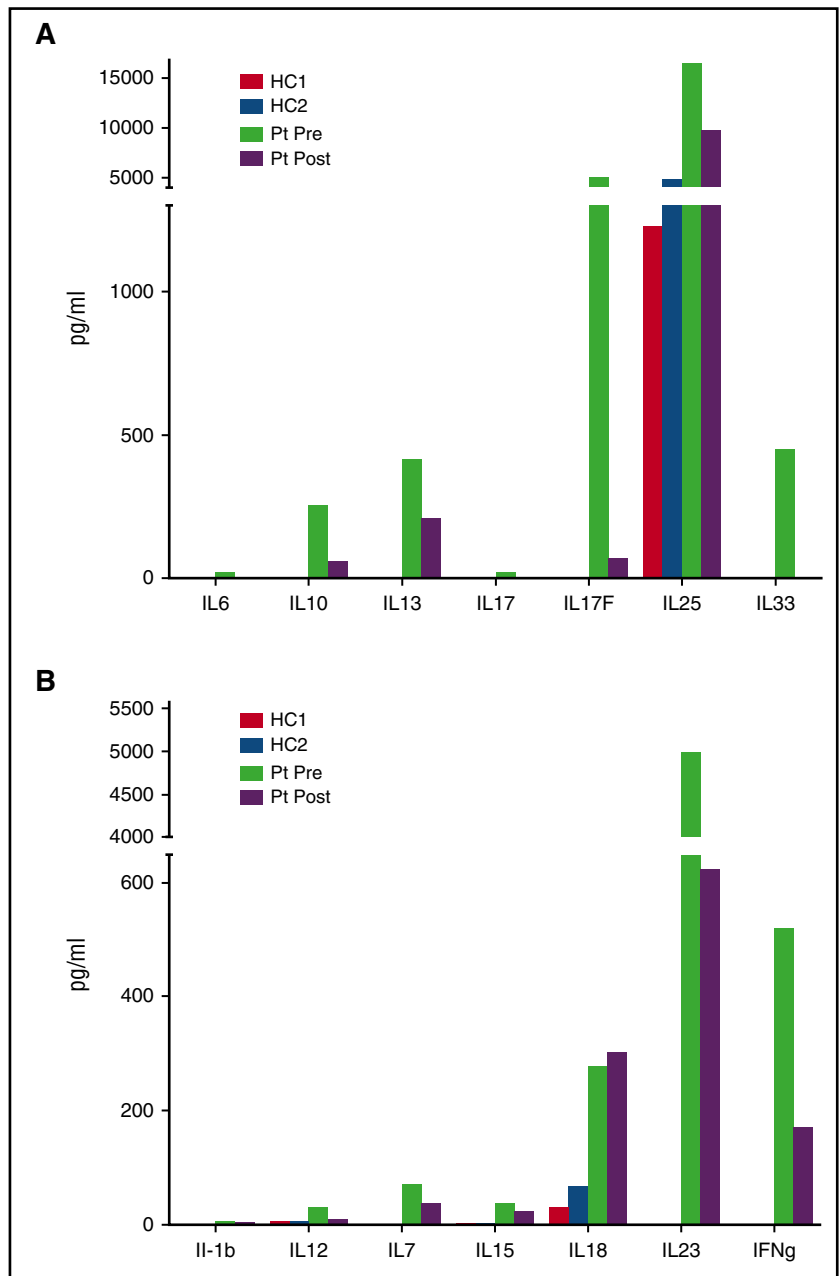
Due to the patient's increasingly aggressive autoinflammatory phenotype, he was referred for consideration of HSCT. No HLA matches were identified within his immediate family. A matched unrelated donor was identified, but transplant was delayed by recurrent attacks of vasculitis, uveitis, and synovitis, during which time the donor was deleted from the registry. Further unrelated donor searches proved unsuccessful.

The clinical picture was further complicated by progressive deterioration in renal function. A renal biopsy was performed, and the biopsy specimen showed features of neutrophil-rich infiltrating tubulointerstitial disease reminiscent of reflux nephropathy, but the patient had no history of recurrent urinary tract infections in childhood. No changes consistent with calcineurin inhibitor toxicity were identified, and no deposition of immunoproteins was observed. Creatinine clearance fell to 24 mL/min. Following the recent success of the GT trial in children, it was suggested that the patient could benefit from treatment using a similar protocol.<sup>14</sup>

WAS severity score prior to GT was 5, reflecting his severe disease phenotype, and hematopoietic cell transplantation–specific comorbidity index score was 8, indicating a high risk of treatment-related mortality.<sup>22</sup> Written informed consent was obtained from the patient after explanation of the risks and benefits and discussion of other treatment options available.

At a follow-up of 20 months post-GT, the patient is well, with normal peripheral blood counts, stable renal function (estimated glomerular filtration rate, 41 mL/min), and no significant episodes of vasculitis or arthritis, and he is free of major immunosuppression. Importantly, he has now completed his education and works part time, neither of which was possible prior to treatment because of his illness. Normal CD4<sup>+</sup>, CD8<sup>+</sup>, and natural killer cell counts were reached at 12 months after therapy (Table 1). T-cell proliferation in response to phytohemagglutinin and

**Figure 5. Reduction in serum cytokine levels post-GT.** Multiple cytokines associated with predominantly lymphoid (A, top) and myeloid (B, bottom) cells were measured by luminex in the patient (Pt) pre- and 18 months post-GT and compared with healthy controls (HC1 and HC2).



anti-CD3/anti-CD28 antibody stimulation also normalized. It should be noted that in addition to an intrinsic suppression as a result of long-standing disease, the patient's pre-GT phytohemagglutinin responses were likely also blunted by the anti-proliferative immunosuppressant mycophenolate mofetil. Long term IVIg supplementation was withdrawn 10 months after gene-therapy as endogenous IgG, IgA, and IgM (5.7, 1.4, and 0.2 g/L, respectively) levels were rising. There was an excellent serological response to tetanus vaccine (Table 1). Response to a single conjugated pneumococcal vaccine (at 22 months post-GT) was partial, with a 10-fold increase in total anti-pneumococcal-specific IgG after 2 vaccinations, but to a restricted repertoire (3/13 serotypes). Platelet counts remained stable, within the normal range after recovery from myelosuppression.

The patient demonstrated robust and multilineage engraftment in peripheral blood of gene-corrected cells, which was sustained to the latest time point analyzed (20 months post-GT). T cells exhibited the

highest level of gene marking at 12 months compared with other lineages as observed in previous studies, although gene marking in myeloid cells was also sustained at ~10%, suggesting that transduced hematopoietic stem cells were successfully engrafted (Figure 1). This was supported by evidence for persistent gene marking in purified bone marrow CD34<sup>+</sup> cells analyzed 16 months after treatment, with an observed vector copy number of 0.34 (Figure 1). B-cell marking was also very robust, as observed in some patients in previous studies (patients 2, 4, and 6 in the study by Hacein-Bey Abina et al<sup>4</sup>). All lineages exhibited restoration of WASp expression (Figure 2A). Western blot analysis confirmed low-level expression of WASp in the platelet fraction at 12 months post-GT, suggesting that a contribution to the platelet compartment was also now derived from engrafted hematopoietic stem cells (Figure 2B). No platelet transfusions were given at any time. Prominent WASp expression was detected in purified naive CD4<sup>+</sup> and CD8<sup>+</sup> T cells at 20 months post-GT (Figure 2C). In

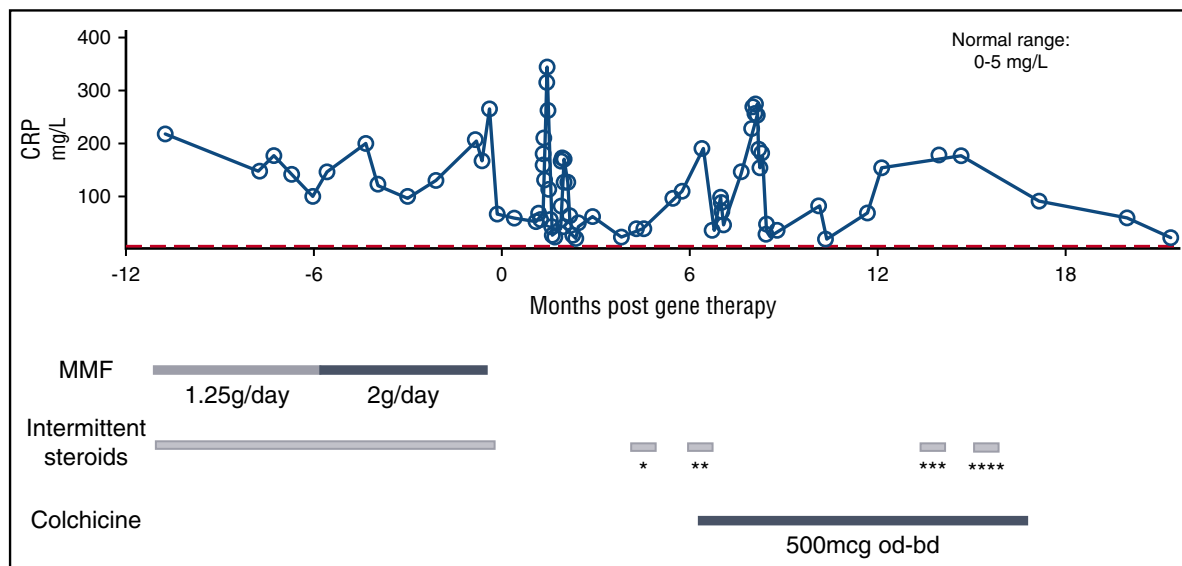


**Figure 6. Clinical course pre- and post-GT showing a reduction in serum C-reactive protein over time.** \*Prednisolone 30 mg daily for 3 days; ankle swelling and cutaneous tenderness, vasculitis (?). \*\*Prednisolone 30 mg daily for 4 days; admitted with lymphadenopathy, pyrexia of unknown origin. \*\*\*Prednisolone 30 mg daily for 3 days; foot swelling and cutaneous tenderness (self-medicated). \*\*\*\*Prednisolone 30 mg daily for 3 days; cutaneous tenderness and nodules (self-medicated). bd, twice daily; CRP, C-reactive protein; MMF, mycophenolate mofetil; od, once daily.

addition, a sustained improvement in T-cell repertoire and thymic output was observed in both CD4<sup>+</sup> and CD8<sup>+</sup> T-cell compartments post-GT (Figure 3A-B).

The distributions of integration site frequencies are summarized in stacked bar graphs in Figure 4. Both the statistics summarized in Table 2 and the stacked bar graphs indicate highly polyclonal cell populations.<sup>23</sup> Low Gini coefficients, high Shannon indices, and high UC50 values (unique cell progenitors contributing the most expanded 50% of progeny cell clones)<sup>15,16</sup> are reported across samples, indicating polyclonality (Table 2). In Figure 4, most of the integration sites sampled are low abundance (colored gray in the figure). No unique clone accounts for >2.5% of the total data for any given sample. Further, no integration site within 100 kb of a gene previously associated with adverse events in GT (*LMO2*, *CCND2*, and *MECOM*) accounts for >0.4% of the total abundance in any cell type at any time point. The polyclonality of integration sites identified in this adult patient is comparable to populations seen in pediatric patients treated with the same vector (LV-w1.6 WASp) at corresponding time points.<sup>14</sup> More detailed analysis of integration site distributions and relative clonal abundance is included in supplemental Figure 2 (available on the *Blood* Web site).

Several short-lived adverse events were noted post-GT, including disseminated shingles (6 months after therapy), transient lymphadenopathy and pyrexia of unknown origin (7 months after therapy), scleritis requiring topical steroids (10 months after therapy), acute acne associated with an inflammatory ulcer on the jawline (supplemental Figure 1), and transient alopecia areata (fungal culture negative). A lymph node biopsy was performed at the time when lymphadenopathy was present, and the biopsy specimen showed reactive changes only. Histology of the inflammatory facial lesion was suggestive of pseudoepitheliomatous hyperplasia with a dense inflammatory infiltrate of lymphocytes, plasma cells, eosinophils, and neutrophils. No atypical mycobacteria or other pathogens were identified, and the lesion resolved with broad-spectrum oral antimicrobial therapy.

In view of his inflammatory disease manifestations, we measured serum cytokine levels pre-GT and 18 months post-GT. Compared with healthy controls, significantly elevated lymphoid- and myeloid-derived

proinflammatory cytokines were observed prior to treatment (Figure 5A-B). Almost all were substantially lower after therapy, although some remained elevated, notably the proinflammatory cytokines IL-18 and interferon- $\gamma$ , which are primarily derived from myeloid cells. Serum C-reactive protein levels, which were very elevated prior to treatment despite mycophenolate mofetil and steroids, also improved over time, possibly enhanced by addition of the anti-inflammatory drug colchicine (Figure 6).

## Discussion

It is reassuring that in this adult patient, the same pattern of reconstitution was observed as seen in pediatric patients (LV-w1.6 WASp),<sup>13,14</sup> suggesting that potential for T-cell repertoire recovery in older patients is well preserved. In keeping with results of previous GT trials gene marking was higher in the lymphoid compared with the myeloid compartment, which is likely due to the previously described survival advantage conferred by WASp expression in mature lymphoid cells in particular.<sup>14,24</sup> This phenomenon has also been observed in WAS patients who have undergone allogeneic HSCT.<sup>7</sup>

The reoccurrence of transitory inflammatory complications post-GT is interesting, as lymphoid reconstitution appears excellent. One episode of acute acne was associated with pseudoepitheliomatous hyperplasia in a facial lesion and bore some resemblance to features of the rare inherited autoinflammatory PAPA (pyogenic arthritis, pyoderma gangrenosum, and acne) syndrome caused by mutations in *PSTPIP1*, a cytoskeletal adaptor known to regulate WASp in macrophages.<sup>25</sup> Both pseudoepitheliomatous hyperplasia and PAPA syndrome are associated with increased production of IL-1B family proinflammatory cytokines, including IL-18.<sup>26,27</sup> It therefore seems likely that there is a persistent inflammasome-mediated mechanism for residual inflammation that may therefore reflect the presence of significant numbers of nontransduced myeloid cells. Interestingly, addition of colchicine successfully suppressed further inflammation.



This is the first report of successful GT in an adult with severe WAS. There was rapid engraftment and expansion of a polyclonal pool of functional T cells and sustained gene marking in myeloid and B-cell lineages up to 20 months of observation. As described, apart from colchicine, the patient was able to discontinue all immunosuppression and has recently been withdrawn from exogenous immunoglobulin support. Longer follow-up and testing in other patients will be required to confirm these early results. Although we recognize that recent developments in reducing the toxicities associated with mismatched allogeneic HSCT may impact on the choice between GT and allogeneic HSCT, the limited side effects associated with the GT procedure and the benefits seen in this case demonstrate that GT using a lentiviral vector may be a viable alternative strategy for adult WAS patients with severe and chronic disease-related complications, for whom an allogeneic HSCT procedure presents an unacceptable risk.

## Acknowledgments

The authors acknowledge support from the Clinical Development Department of Genethon, notably that of G. Honnet, M. L. Gourlay-Chu, and V. Delahais.

E.C.M. and S.O.B. are supported by the UCL Hospitals National Institute for Health Research Biomedical Research Centre. The study is sponsored by Genethon, which is supported by funds from

AFM/Telethon and the French Muscular Dystrophy Association. A.J.T. is supported by the Wellcome Trust (104807/Z/14/Z). The study was also supported by the National Institute for Health Research Biomedical Research Centre at Great Ormond Street Hospital for Children NHS Foundation Trust and University College London.

## Authorship

Contribution: E.C.M., S.O.B., T.F., and A.J.T. analyzed the data and wrote the manuscript; E.C.M. and A.J.T. were clinical trial principal and chief investigators; S.W., S.G., R. Chee, A.D.S., R. Chakraverty, E.C.M., and S.O.B. provided clinical care of the patient; R.T. was the trial coordinator; H.H., C.D., K.S., C.R., K.G., K. Butler, K. Buckland, H.B.G., and A.J.T. manufactured the GT product; A.G. and F. Mavilio were representatives of the vector manufacturer and of the study sponsor; F.D.B. and F. Male performed integration site analysis; H.I. performed histopathological analysis; and A.G., H.B.G., and A.J.T. were involved in trial design.

Conflict-of-interest disclosure: The authors declare no competing financial interests.

Correspondence: Emma C. Morris, UCL Institute of Immunity and Transplantation, 2nd floor, Royal Free London Hospital, Rowland Hill St, London NW3 2PF, United Kingdom; e-mail: e.morris@ucl.ac.uk.

## References

- Thrasher AJ, Burns SO. WASP: a key immunological multitasker. *Nat Rev Immunol*. 2010;10(3):182-192.
- Baptista MA, Keszei M, Oliveira M, et al. Deletion of Wiskott-Aldrich syndrome protein triggers Rac2 activity and increased cross-presentation by dendritic cells. *Nat Commun*. 2016;7:12175.
- Burns S, Cory GO, Vainchenker W, Thrasher AJ. Mechanisms of WASp-mediated hematologic and immunologic disease. *Blood*. 2004;104(12):3454-3462.
- Meyer-Bahlburg A, Becker-Herman S, Humblet-Baron S, et al. Wiskott-Aldrich syndrome protein deficiency in B cells results in impaired peripheral homeostasis. *Blood*. 2008;112(10):4158-4169.
- Worth AJ, Thrasher AJ. Current and emerging treatment options for Wiskott-Aldrich syndrome. *Expert Rev Clin Immunol*. 2015;11(9):1015-1032.
- Zhu Q, Zhang M, Blaese RM, et al. The Wiskott-Aldrich syndrome and X-linked congenital thrombocytopenia are caused by mutations of the same gene. *Blood*. 1995;86(10):3797-3804.
- Pai SY, DeMartis D, Forino C, et al. Stem cell transplantation for the Wiskott-Aldrich syndrome: a single-center experience confirms efficacy of matched unrelated donor transplantation. *Bone Marrow Transplant*. 2006;38(10):671-679.
- Pai SY, Notarangelo LD. Hematopoietic cell transplantation for Wiskott-Aldrich syndrome: advances in biology and future directions for treatment. *Immunol Allergy Clin North Am*. 2010;30(2):179-194.
- Moratto D, Gilliani S, Bonfim C, et al. Long-term outcome and lineage-specific chimerism in 194 patients with Wiskott-Aldrich syndrome treated by hematopoietic cell transplantation in the period 1980-2009: an international collaborative study. *Blood*. 2011;118(6):1675-1684.
- Kharya G, Nademi Z, Leahy TR, et al. Haploidentical T-cell alpha beta receptor and CD19-depleted stem cell transplant for Wiskott-Aldrich syndrome. *J Allergy Clin Immunol*. 2014;134(5):1199-1201.
- Locatelli F, Bauquet A, Palumbo G, Moretta F, Bertina A. Negative depletion of  $\alpha/\beta$  T cells and of CD19+ B lymphocytes: a novel frontier to optimize the effect of innate immunity in HLA-mismatched hematopoietic stem cell transplantation. *Immunol Lett*. 2013;155(1-2):21-23.
- Braun CJ, Boztug K, Paruzynski A, et al. Gene therapy for Wiskott-Aldrich syndrome: long-term efficacy and genotoxicity. *Sci Transl Med*. 2014;6(227):227ra33.
- Aiuti A, Biasco L, Scaramuzza S, et al. Lentiviral hematopoietic stem cell gene therapy in patients with Wiskott-Aldrich syndrome. *Science*. 2013;341(6148):1233-151.
- Hacein-Bey Abina S, Gaspar HB, Blondeau J, et al. Outcomes following gene therapy in patients with severe Wiskott-Aldrich syndrome. *JAMA*. 2015;313(15):1550-1563.
- Sherman E, Nobles C, Berry CC, et al. INSPIRED: a pipeline for quantitative analysis of sites of new DNA integration in cellular genomes. *Mol Ther Methods Clin Dev*. 2017;4:39-49.
- Berry CC, Nobles C, Six E, et al. INSPIRED: quantification and visualization tools for analyzing integration site distributions. *Mol Ther Methods Clin Dev*. 2016;4:17-26.
- Berry C, Hannenhalli S, Leipzig J, Bushman FD. Selection of target sites for mobile DNA integration in the human genome. *PLoS Comput Biol*. 2006;2(11):e157.
- Berry CC, Ocwieja KE, Malani N, Bushman FD. Comparing DNA integration site clusters with scan statistics. *Bioinformatics*. 2014;30(11):1493-1500.
- Berry CC, Gillet NA, Melamed A, Gormley N, Bangham CR, Bushman FD. Estimating abundances of retroviral insertion sites from DNA fragment length data. *Bioinformatics*. 2012;28(6):755-762.
- Zhu Q, Watanabe C, Liu T, et al. Wiskott-Aldrich syndrome/X-linked thrombocytopenia: WASP gene mutations, protein expression, and phenotype. *Blood*. 1997;90(7):2680-2689.
- Jin Y, Mazza C, Christie JR, et al. Mutations of the Wiskott-Aldrich syndrome protein (WASP): hotspots, effect on transcription, and translation and phenotype/genotype correlation. *Blood*. 2004;104(13):4010-4019.
- Sorror ML, Maris MB, Storb R, et al. Hematopoietic cell transplantation (HCT)-specific comorbidity index: a new tool for risk assessment before allogeneic HCT. *Blood*. 2005;106(8):2912-2919.
- Chao A. Estimating the population size for capture-recapture data with unequal catchability. *Biometrics*. 1987;43(4):783-791.
- Westerberg LS, de la Fuente MA, Wermeling F, et al. WASP confers selective advantage for specific hematopoietic cell populations and serves a unique role in marginal zone B-cell homeostasis and function. *Blood*. 2008;112(10):4139-4147.
- Starnes TW, Bennis DA, Bing X, et al. The F-BAR protein PSTPIP1 controls extracellular matrix degradation and filopodia formation in macrophages. *Blood*. 2014;123(17):2703-2714.
- Ristow HJ. A major factor contributing to epidermal proliferation in inflammatory skin diseases appears to be interleukin 1 or a related protein. *Proc Natl Acad Sci USA*. 1987;84(7):1940-1944.
- Marzano AV, Borghi A, Meroni PL, Cugno M. Pyoderma gangrenosum and its syndromic forms: evidence for a link with autoinflammation. *Br J Dermatol*. 2016;175(5):882-891.